Elsevier Editorial System(tm) for Materials Characterization
Manuscript Draft

Manuscript Number:

Title: In-situ small-angle X-ray scattering study of the precipitation behavior in a Fe-25at%Co-9at%Mo alloy

Article Type: Short Communication

Keywords: Fe-Co-Mo alloy; intermetallic phases; precipitation; synchrotron radiation; small-angle X-ray scattering

Corresponding Author: Dr. Gerald A Zickler, Ph.D.

Corresponding Author's Institution: University of Leoben

First Author: Gerald A Zickler, Ph.D.

Order of Authors: Gerald A Zickler, Ph.D.; Elisabeth Eidenberger; Harald Leitner; Erich Stergar; Helmut Clemens; Peter Staron; Thomas Lippmann; Andreas Schreyer

In-situ small-angle X-ray scattering study of the precipitation behavior in a Fe-25at%Co-9at%Mo alloy

Gerald A. Zickler[a,b,1], Elisabeth Eidenberger[a], Harald Leitner[a,b], Erich Stergar[a], Helmut Clemens[a], Peter Staron[c], Thomas Lippmann[c], and Andreas Schreyer[c]

[a] Department of Physical Metallurgy and Materials Testing, Montanuniversität Leoben, Franz-Josef-Straße 18, A-8700 Leoben, Austria

[b] Christian Doppler Laboratory for Early Stages of Precipitation, Montanuniversität Leoben, Franz-Josef-Straße 18, A-8700 Leoben, Austria

[c] GKSS Research Center Geesthacht, Max-Planck-Straße 1, D-21502 Geesthacht, Germany

[1] Corresponding author. Tel.: +43 3842 4024206; Fax: +43 3842 4024202. E-mail address: gerald.zickler@mu-leoben.at (G. A. Zickler)

In-situ small-angle X-ray scattering study of the precipitation behavior in a Fe-25at%Co-9at%Mo alloy

Gerald A. Zickler[a,b,*], Elisabeth Eidenberger[a], Harald Leitner[a,b], Erich Stergar[a], Helmut Clemens[a], Peter Staron[c], Thomas Lippmann[c], and Andreas Schreyer[c]

[a] Department of Physical Metallurgy and Materials Testing, Montanuniversität Leoben, Franz-Josef-Straße 18, A-8700 Leoben, Austria

[b] Christian Doppler Laboratory for Early Stages of Precipitation, Montanuniversität Leoben, Franz-Josef-Straße 18, A-8700 Leoben, Austria

[c] GKSS Research Center Geesthacht, Max-Planck-Straße 1, D-21502 Geesthacht, Germany

[*] Corresponding author. Tel.: +43 3842 4024206; Fax: +43 3842 4024202. E-mail address: gerald.zickler@mu-leoben.at (G. A. Zickler)

Abstract

Fe-Co-Mo alloys show extraordinary mechanical properties which make them potential candidates for various high-performance applications. In the present study, for the first time, the precipitation behavior in a Fe-25at%Co-9at%Mo alloy was studied by small-angle X-ray scattering using high-energy synchrotron radiation. The specimens were isothermally aged in an *in-situ* furnace. The small-angle X-ray scattering patterns showed scaling behavior and were evaluated by employing a model function from the literature. This approach provides information about the characteristic length scale and the volume fraction of the precipitates in the alloy.

Keywords: Fe-Co-Mo alloy; Intermetallic phases; Precipitation; Synchrotron radiation; Small-angle X-ray scattering.

Introduction

Despite the fact that the first studies on the ternary Fe-Co-Mo alloy system were performed many years ago [1], only little is known about the prevailing phases and their formation in the system. Fe-Co-Mo alloys show a characteristic hardening mechanism, which is characterized by low hardness in the solution annealed state and a significant increase of hardness up to 70 Rockwell C during subsequent aging treatments [2]. These extraordinary mechanical properties make the alloy a potential candidate for various high-performance applications. It is assumed that the strengthening is caused by precipitation of the nanometer-sized intermetallic μ phase from a supersaturated matrix [3]. In the Fe-Co-Mo phase diagram, the μ phase field completely traverses the ternary system from $(Co,Mo)_{\mu}$ to $(Fe,Mo)_{\mu}$ [4]. Thus the μ phase is assigned the chemical composition $(Fe,Co)_7Mo_6$ as a mixture of the two rhombohedral phases Co_7Mo_6 [5] and Fe_7Mo_6 [6]. In a recent study, atom probe field ion microscopy was applied for investigating the precipitation behavior in the Fe-25at%Co-9at%Mo alloy, yielding detailed real-space information on a very local scale [7]. The investigation showed that the precipitation starts with the diffusion of Mo, followed by the formation of the intermetallic μ phase.

Small-angle scattering is a powerful method for providing quantitative and statistically relevant data for the characterization of size, shape, volume fraction, and arrangement of nanometer-sized second phase particles in hard condensed matter [8-11]. Especially high-energy X-rays, such as provided by modern synchrotron radiation sources bear the advantage of high photon brilliance and low absorption in most

materials [12], enabling time-resolved *in-situ* measurements of phase transformations in bulk materials. *In-situ* small-angle X-ray scattering (SAXS) using synchrotron radiation supplies deeper information of the precipitation behavior in metallic alloys, particularly focusing on the early stages of precipitation kinetics. The beginning and the end of the precipitation reactions are of great theoretical and technological interest, since they especially determine the mechanical properties of the material.

The ternary alloy Fe-Co-Mo represents an ideal system for studying the precipitation behavior by *in-situ* SAXS. In the present study, for the first time SAXS using high-energy synchrotron radiation was applied for *in-situ* studies of the precipitation behavior in a Fe-Co-Mo alloy. These *in-situ* SAXS experiments allow following the kinetics of precipitation at different aging temperatures in a relative short time, yielding eventually a statistically relevant measure for size and volume fraction of the precipitated phase.

Experimental

The chemical composition of the ternary Fe-Co-Mo alloy investigated is given by: Fe base, 25.1 at% Co, 9.3 at% Mo, 0.4 at% Si, and 0.1 at% C [7]. The material was machined to cylindrical samples with a diameter of 5 mm and a length of 15 mm. The specimens were solution annealed at 1453 K for 5 min in a quenching dilatometer Bähr 805 A/D.

The *in-situ* high-energy SAXS studies of the precipitation kinetics in the Fe-Co-Mo alloy were performed at the Engineering Materials Science Beamline HARWI-II [13] at the GKSS outstation at the Deutsches Elektronen-Synchrotron (DESY) in

Hamburg, Germany. For the experiment, a custom-made high-temperature furnace was used [14], which consists of a water-cooled socket and an evacuated sphere of quartz glass. The heating element is a strip of carbon foil, which is bent in an arc over the specimen. A Lake Shore 340 temperature controller (Lake Shore Cryotronics, Westerville, OH, USA) was used for temperature control of the furnace. The cylindrical sample was screwed on the sample holder, which was equipped with a K-type thermocouple, providing the temperature in the core of the specimen. The position of measurement was 1 mm above the thermocouple. The samples were heated up with a rate of 100 K min^{-1} and isothermally aged at 698, 723, 748, and 773 K, respectively. Monochromatic synchrotron radiation with a nominal energy of 100 keV was used for the SAXS experiments. The cross-section of the primary beam at the sample position was defined by a series of slit apertures to 0.5 × 0.5 mm^2. SAXS patterns were taken continuously during isothermal aging as function of time t, where the maximum aging time was 9297 s at 698 K, 10806 s at 723 K, 4751 s at 748 K, and 4451 s at 773 K. A two-dimensional image plate detector (mar345, Marresearch, Norderstedt, Germany) with a resolution of 2300 × 2300 pixels (pixel size: 150 × 150 μm^2) at a sample-to-detector distance of 9.8 m was used to detect the scattered photons. An exposure time of 210 s was used for each measurement. The SAXS patterns covered a range of scattering vector of 0.2 $nm^{-1} < q < 5.0\ nm^{-1}$, where the length of the scattering vector is given by $|\mathbf{q}| = q = (4\pi / \lambda) \sin\theta$, with 2θ being the scattering angle and λ the wavelength. The SAXS patterns were normalized to the primary intensity of the synchrotron X-ray flux and suitable corrected for parasitic background scattering, electronic noise, transmission, and polarization by using the data reduction program FIT2D [15]. No calibration to absolute intensity was performed. All measurements showed radial

isotropic scattering intensity which was azimuthally averaged for equal radial distances from the central beam.

Results and discussion

Figure 1 shows typical azimuthally averaged scattering intensity $I(q,t)$ for the investigated ternary Fe-Co-Mo alloy in the solution annealed and differently aged states. The given aging times correspond to the end of the exposure of the detector. The shown examples are exemplarily for all measured SAXS curves. The as-quenched sample shows a continuous decrease of scattering intensity with increasing q and it reaches a constant value at larger q, indicating that the material is well homogenized. The scattering intensity of the as-quenched sample is attributed to rather large inhomogeneities such as grain boundaries and various impurities. A considerable increase of the scattering intensity is already observed after aging at 698 K, where a growing maximum shifts from 2.4 nm^{-1} at the early stages to 1.3 nm^{-1} in the investigated time range (Figure 1a). As seen in Figure 1, the trends in the aging series at all four temperatures are qualitatively similar. At all temperatures investigated, the scattering intensity at small q seems to be unaffected by the aging treatment.
It is assumed that $I(q,t)$ is an incoherent superposition of the individual scattering contributions of rather large inhomogeneities (scattering intensity at small q) and precipitates (characteristic peak maximum). Therefore, the SAXS patterns of the as-quenched specimens of each aging series were least-square fitted at very small q values by $I(q,t) = C\, q^{-n}$, where C as a pre-factor and n is the slope of measured scattering intensity in a double logarithmic plot, in order to subtract the fitted scattering

contributions from each SAXS curve of the aged material. The constant scattering (Laue scattering) at large q was subtracted from each SAXS curve individually by performing a Porod analysis according to the references [16,17].

Due to the fact that the scattering intensity is not on absolute scale, a scaling model was used for the evaluation of the SAXS patterns. Fratzl *et al*. [18-20] proposed a heuristic structure function $S(q,t)$ for modeling of phase separations, where the surface energy provides the only driving force. The model describes various morphologies of the precipitates reaching from isolated clusters to interconnected rods or plates. It contains only one fitting parameter γ, which is defined as [19]

$$\gamma = \frac{\sigma D}{8\pi \phi(1-\phi)}, \qquad (1)$$

where σ is the interfacial area per unit volume, D represents the domain size, and ϕ is the volume fraction of the second phase. The parameter γ is inverse proportional to the width of the scaled structure function $S(q,t) / S(q_m(t),t)$. So far the scaling function was used for modeling small-angle scattering data for various metallic alloys [19-22].
The remaining scattering intensity is attributed as structure function $S(q,t)$ [18,19,23] of the precipitates. $S(q,t)$ has its maximum at the scattering vector $q_m(t)$, which is in inverse proportion to the characteristic length scale $2\pi / q_m(t)$ in the sample [18, 23]. Figure 2 displays the variation of $2\pi / q_m(t)$ as function of aging time for various temperatures. Obviously the characteristic length scale shows a simple power law behavior $(2\pi/q_m) \propto t^a$. The values of the exponent a were derived as 0.18 at 698 K, 0.24 at 723 K, 0.23 at 748 K, and 0.25 at 773 K. The explanation for the determined exponents could be competing mechanisms in the microstructural development, e.g. cluster

coagulation would provide an exponent of 0.2 [24]. Similar trends were observed in Fe-Cr alloys, where exponents between 0.13 and 020 were found [25,26].

The scaled structure function $S(q,t) / S(q_m(t),t)$ [18-20] is plotted *versus* $q/q_m(t)$ in Figure 3, showing that the curves are almost identical despite the width of the curve. For 698 K (Figure 3a) the width of the scaling functions becomes slightly smaller with increasing aging time. For higher aging temperatures the dependence on time is rather weak. As shown in Figure 3, the measured structure functions of the ternary Fe-Co-Mo alloy could be successfully fitted by the model scaling function. For all four aging temperatures, γ rapidly decreases to a steady state of about 0.45 in the investigated time range. By applying equation (1), γ is related to ϕ by $\gamma = \left[2(4\pi/3)^{2/3}\phi^{1/3}(1-\phi)\right]^{-1}$ for spherical morphology and $\gamma = \left[4\pi^{1/2}\phi^{1/2}(1-\phi)\right]^{-1}$ for rod-like morphology [20]. At $\gamma \approx$ 0.42 the scaling model shows a transition from the spherical towards the rod-like case, which means that in this regions both morphologies are possible [20]. Presently atom probe field ion microscopy and transmission electron microscopy investigations are in progress in order to identify the exact precipitate morphology. However, a rough estimate for the volume fraction can be made, providing $\phi \approx 0.11$ (spheres) or $\phi \approx 0.13$ (rods). When discussing absolute values of ϕ one should keep in mind, that Fratzl and Lebowitz postulated that their model only obtains the value of ϕ correctly within 10% [20]. Furthermore, one should bear in mind that the accuracy of the width of the scaled structure function is not high, because of noisy data, especially at the high-q flank of $S(q,t)$.

Summary

The precipitation behavior in the ternary Fe-25at%Co-9at%Mo during isothermal aging was studied. SAXS using high-energy synchrotron radiation was applied for *in-situ* aging experiments to follow the kinetics of precipitation. The SAXS patterns were evaluated by using a scaled structure function which yields the characteristic length scale and volume fraction of the precipitates. Despite the fact that the precipitation kinetics was studied *in-situ*, the interpretation of the early stages are critical due to the finite heating rate of 100 K min^{-1} and the relative long exposure time of the detector. In conclusion, *in-situ* SAXS using synchrotron radiation supplies deeper information on the precipitation behavior, especially focusing on the early stages of precipitation. However, detailed investigations of the very early stages would need fast detectors with shorter readout times, which should be available for forthcoming investigations.

Acknowledgements

The authors thank T. Fischer for providing assistance at the synchrotron beamline and R. Nowak for technical support with the *in-situ* furnace. Financial support from the Deutsches Elektronen-Synchrotron (DESY) and the European Community (reimbursement contract RII3-CT-2004-506008 (IA-SFS)) is gratefully acknowledged.

References

1. Köster W, Tonn W. Das System Eisen-Kobalt-Molybdän. Arch Eisenhüttenwes 1932;5:627-30.

2. Köster W. Mechanische und magnetische Ausscheidungshärtung der Eisen-Kobalt-Wolfram- und Eisen-Kobalt-Molybdän-Legierungen. Arch Eisenhüttenwes 1932;6:17-23.

3. Geller Y. Tool Steels. Moscow: Mir Publishers; 1978.

4. Das DK, Rideout SP, Beck PA. Intermediate phases in the Mo-Fe-Co, Mo-Fe-Ni, and Mo-Ni-Co ternary systems. J Met 1952;4:1071-5.

5. Forsyth JB, d′Alte da Veiga LM. The structure of the μ-phase Co_7Mo_6. Acta Cryst 1962;15:543-6.

6. Baen SR, Duwez P. Constitution of iron-chromium-molybdenum alloys at 1200°F. J Met 1951;3:331-5.

7. Leitner H, Schober M, Clemens H, Caliskanoglu D, Danoix F. Precipitation behaviour of a Fe-Co-Mo-alloy during non-isothermal aging. Int J Mater Res 2008 accepted for publication.

8. Kostorz G. Small-angle scattering studies of phase separation and defects in inorganic materials. J Appl Cryst 1991;24:444-56.

9. Fratzl P. Small-angle scattering in materials science – a short review of applications in alloys, ceramics and composite materials. J Appl Cryst 2003;36:397-404.

10. Leitner H, Bischof M, Clemens H, Erlach S, Sonderegger B, Kozeschnik E, Svoboda J, Fischer FD. Precipitation behaviour of a complex steel. Adv Eng Mater 2006;8:1066-77.

11. Simon J-P. Contribution of synchrotron radiation to small-angle X-ray scattering studies in hard condensed matter. J Appl Cryst 2007;40:s1-9.

12. Liss K-D, Bartels A, Schreyer A, Clemens H. High-energy X-rays: a tool for advanced bulk investigations in materials science and physics. Texture Microstruct 2003;35:219-52.

13. Lippmann T, Lottermoser L, Beckmann F, Martins RV, Dose T, Kirchhof R, Schreyer A. New developments at the engineering materials science beamline HARWI-II. In Caliebe W, Drube W, Rickers, K, Schneider JR, editors. HASYLAB Annual Report. Hamburg: HASYLAB/DESY; 2007, p. 113-7.

14. von Zimmermann M, Nowak R, In Schneider JR, editor. HASYLAB Annual Report. Hamburg: HASYLAB/DESY; 2004, p. 100.

15. Hammersley AP, Svensson SO, Hanfland M, Fitch AN, Häusermann D. Two-dimensional detector software: from real detector to idealised image or two-theta scan. High Press Res 1996;14:235-48.

16. Porod G. Die Röntgenkleinwinkelstreuung von dichtgepackten kolloiden Systemen. Kolloid-Z 1951;124:83-114.

17. Porod G. Die Röntgenkleinwinkelstreuung von dichtgepackten kolloiden Systemen. Kolloid-Z 1952;125:51-122.

18. Fratzl P, Lebowitz JL, Penrose O, Amar J. Scaling function, self-similarity, and the morphology of phase-separating systems. Phys Rev B 1991;44:4794-811

19. Fratzl P. Volume-fraction dependence of the scaling function for phase-separating systems. J Appl Cryst 1991;24:593-7.

20. Fratzl P, Lebowitz JL. Universality of scaled structure functions in quenched systems undergoing phase separation. Acta Metall 1989;37:3245-8.

21. Langmayr F, Fratzl P, Vogl G. Volume fraction dependence of the structure function in aged Al-Ag. Acta Metall Mater 1992;40:3381-7.

22. Zickler GA, Tian B, Lind C, Paris O. Separation of scattering contributions from carbides and γ' precipitates in Nimonic 80a by combining small-angle X-ray and neutron scattering. J Appl Cryst 2003;36:484-8.

23. Binder K, Fratzl P. Spinodal decomposition. In: G. Kostorz, editor. Phase transformations in materials, Weinheim: Wiley-VCH; 2001, p. 409-80.

24. Fratzl P, Penrose O. Competing mechanisms for precipitate coarsening in phase separation with vacancy dynamics. Phys Rev B 1997;55:R6101-4.

25. Katano S, Iizumi M. Crossover phenomena in dynamical scaling of phase separation in Fe-Cr alloy. Phys Rev Lett 1984;52:835-8.

26. Furusaka M, Ishikawa Y, Yamaguchi S, Fujino Y. Phase separation process in FeCr alloys studied by neutron small angle scattering. J Phys Soc Japan 1986;55:2253-69.

High-resolution Figure(s) 1

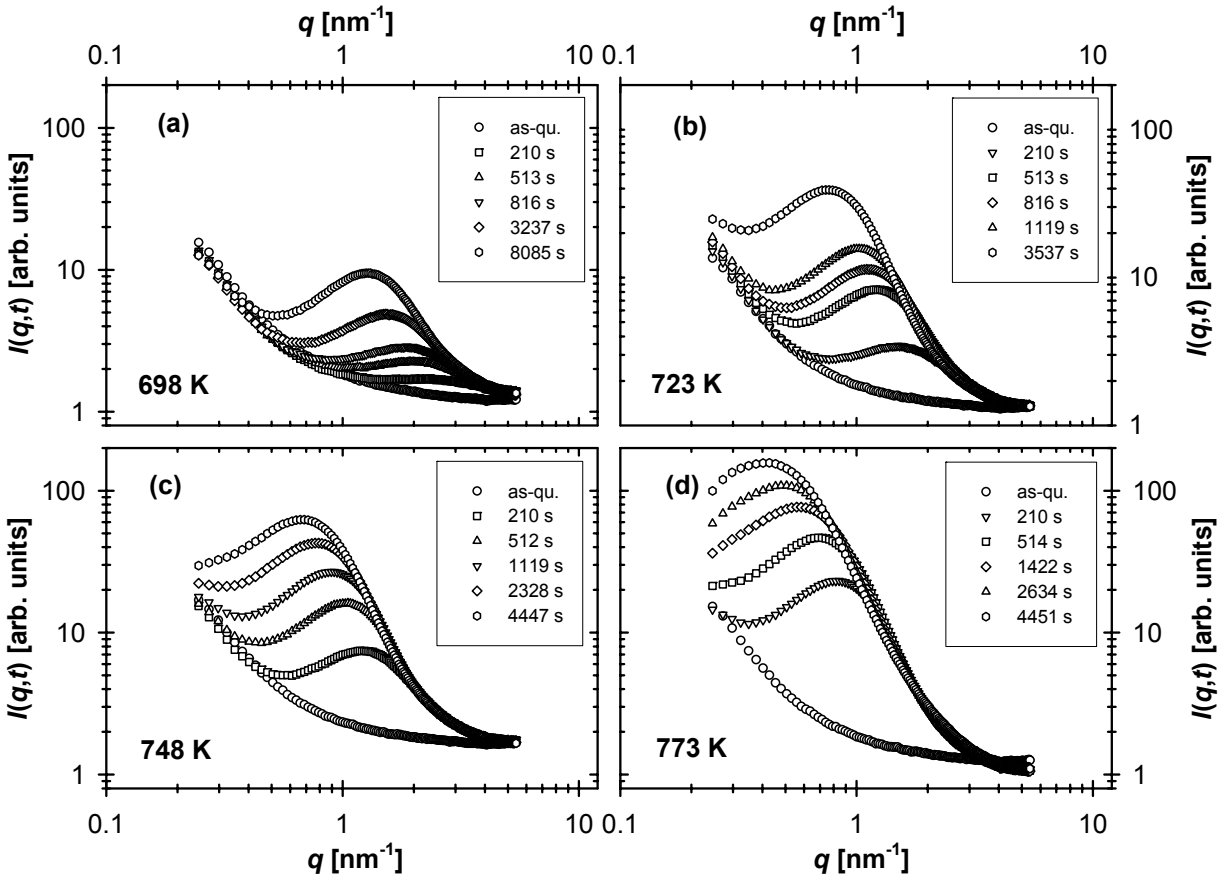

High-resolution Figure(s) 2

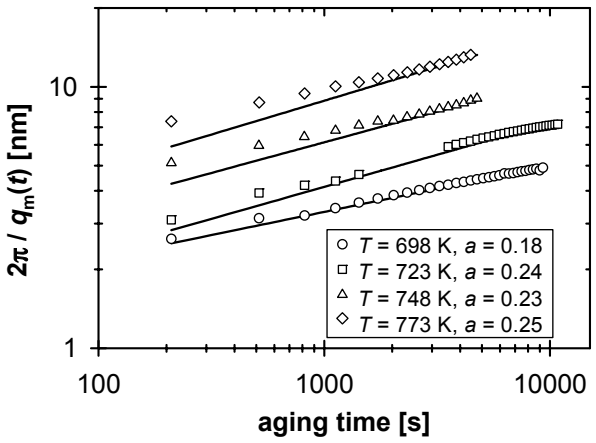

High-resolution Figure(s) 3

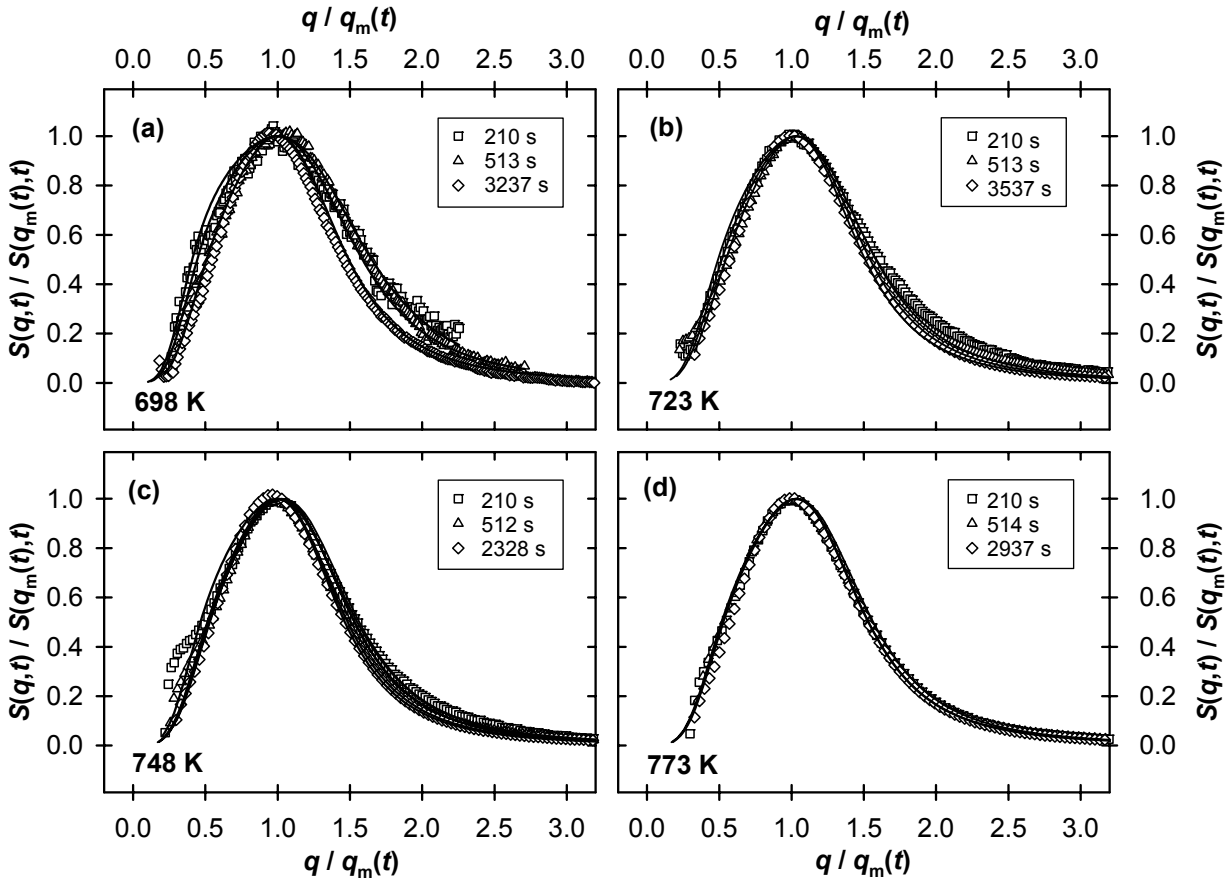

Figures captions

Figure 1: Azimuthally averaged scattering intensity $I(q,t)$ for the ternary Fe-Co-Mo alloy in the as-quenched state and isothermally aged at (a) 698, (b) 723, (c) 748, and (d) 773 K for various times (see figure legend).

Figure 2: The variation of $2\pi / q_{\mathrm{m}}$ of the ternary Fe-Co-Mo alloy as function of aging time for various temperatures. The solid lines denote fitting of the data by $\left(2\pi/q_{\mathrm{m}}\right) \propto t^{\mathrm{a}}$. The derived values of the exponent *a* are shown in the figure legend.

Figure 3: The scaled structure function $S(q,t) / S(q_{\mathrm{m}}(t),t)$ for the ternary Fe-Co-Mo alloy isothermally aged at (a) 698, (b) 723, (c) 748, and (d) 773 K for various times (see figure legends). The solid lines represent the least-square fitted scaling function of Fratzl *et al*. [18].